Received: 13 January 2016 | Accepted: 25 August 2016

DOI: 10.1111/gbi.12215

ORIGINAL ARTICLE

WILEY gebiology

Groundwater shapes sediment biogeochemistry and microbial diversity in a submerged Great Lake sinkhole

L. E. Kinsman-Costello[1] | C. S. Sheik[2] | N. D. Sheldon[3] | G. Allen Burton[4] | D. M. Costello[1] | D. Marcus[3,*] | P. A. Den Uyl[3,†] | G. J. Dick[3]

[1]Department of Biological Sciences, Kent State University, Kent, OH, USA

[2]Department of Biology, Large Lakes Observatory, University of Minnesota Duluth, Duluth, MN, USA

[3]Department of Earth and Environmental Sciences, University of Michigan, Ann Arbor, MI, USA

[4]School of Natural Resources and the Environment, University of Michigan, Ann Arbor, MI, USA

Correspondence

L. E. Kinsman-Costello, Department of Biological Sciences, Kent State University, Kent, OH, USA.
Email: lkinsman@kent.edu

Present addresses:
*Department of Microbiology & Biophysics, The Ohio State University, Columbus, OH, USA
†The Research Corporation of the University of Hawaii, Honolulu, Washington, HI, USA

Abstract

For a large part of earth's history, cyanobacterial mats thrived in low-oxygen conditions, yet our understanding of their ecological functioning is limited. Extant cyanobacterial mats provide windows into the putative functioning of ancient ecosystems, and they continue to mediate biogeochemical transformations and nutrient transport across the sediment–water interface in modern ecosystems. The structure and function of benthic mats are shaped by biogeochemical processes in underlying sediments. A modern cyanobacterial mat system in a submerged sinkhole of Lake Huron (LH) provides a unique opportunity to explore such sediment–mat interactions. In the Middle Island Sinkhole (MIS), seeping groundwater establishes a low-oxygen, sulfidic environment in which a microbial mat dominated by *Phormidium* and *Planktothrix* that is capable of both anoxygenic and oxygenic photosynthesis, as well as chemosynthesis, thrives. We explored the coupled microbial community composition and biogeochemical functioning of organic-rich, sulfidic sediments underlying the surface mat. Microbial communities were diverse and vertically stratified to 12 cm sediment depth. In contrast to previous studies, which used low-throughput or shotgun metagenomic approaches, our high-throughput 16S rRNA gene sequencing approach revealed extensive diversity. This diversity was present within microbial groups, including putative sulfate-reducing taxa of *Deltaproteobacteria*, some of which exhibited differential abundance patterns in the mats and with depth in the underlying sediments. The biological and geochemical conditions in the MIS were distinctly different from those in typical LH sediments of comparable depth. We found evidence for active cycling of sulfur, methane, and nutrients leading to high concentrations of sulfide, ammonium, and phosphorus in sediments underlying cyanobacterial mats. Indicators of nutrient availability were significantly related to MIS microbial community composition, while LH communities were also shaped by indicators of subsurface groundwater influence. These results show that interactions between the mats and sediments are crucial for sustaining this hot spot of biological diversity and biogeochemical cycling.

 © 2016 John Wiley & Sons Ltd

1 | INTRODUCTION

In the distant past, cyanobacteria-dominated microbial mats were the dominant forms of life, and are believed to have flourished in low-oxygen environments lacking multicellular grazers and herbivores (Matheron & Caumette, 2015). Cyanobacterial mat metabolic activity shaped biogeochemical cycles in the Precambrian and drove major turning points in the geochemical evolution of Earth's surface (Hayes & Waldbauer, 2006; Hoehler, Bebout, & Des Marais, 2001). Although mats in coastal oceans are often assumed to be the agents of such global change, recent work suggests that terrestrial and freshwater cyanobacterial mats may have played a critical role in Earth's oxygenation (Lalonde & Konhauser, 2015). Under certain conditions, benthic mats proliferate on the sediment surface in modern aquatic ecosystems (Stal, 1995), where they are powerful engineers of ecosystem condition and biogeochemical function (Canfield & Des Marais, 1993; Paerl, Pinckney, & Steppe, 2000). In these modern, sometimes extreme, environments, mat consortia provide insight into how living organisms shape the biogeochemistry of our planet, both now and in the distant past (Paerl et al., 2000; Sumner, Hawes, Mackey, Jungblut, & Doran, 2015).

Benthic microbial mat communities are tightly linked to the microbial communities in underlying sediments. Photosynthetic mats stabilize surface sediments (Decho, 1990) and exude labile organic substrates, which in turn fuel heterotrophic microbial metabolism, establishing physicochemical gradients of oxygen concentration, pH, and redox potential. These sharp gradients are strengthened and maintained by the physical structure of mat communities, which slows molecular diffusion and prevents movement of particles across the sediment–water interface (Paerl et al., 2000; Stal, 1995). Together these physical and chemical effects of microbial mats influence biogeochemical cycling, especially the mobility of metals and nutrients across the sediment–water interface (Battin, Kaplan, Newbold, & Hansen, 2003; Nimick et al., 2003). Sediments beneath microbial mats, which are typically organic-rich, serve as a reservoir and source of nutrients that fuel mat growth and function, a role that may be especially important to mats that live in low-nutrient waters (Matheron & Caumette, 2015). When disturbance from grazing and bioturbating animals is limited, resources supplied from underlying sediment may be the dominant control over mat structure and function.

In the absence of oxygen, the sediment environment supports alternative terminal electron-accepting process, such as iron and sulfate (SO_4^{2-}) reduction, fermentation, and methanogenesis (Schlesinger & Bernhardt, 2013). By-products of complex organic matter breakdown and fermentation fuel SO_4^{2-}-reducing micro-organisms (Megonigal, Hines, & Visscher, 2004), and in turn, the sulfide produced can then be used to drive two forms of primary production: anoxygenic photosynthesis and sulfide oxidation (Matheron & Caumette, 2015; Voorhies et al., 2012). Methanogenesis in deep organic sediments provides an energy source for methanotrophic organisms, supports carbon breakdown in anoxic environments that lack other terminal electron acceptors, and produces a highly potent greenhouse gas (Megonigal et al., 2004; Schlesinger & Bernhardt, 2013). Despite the importance of sediment microbial communities and geochemistry, underlying sediments are often overlooked when characterizing benthic microbial mat ecosystems.

Submerged groundwater seeps in karst sinkholes of the Laurentian Great Lakes establish chemically distinct ecosystems, where unique benthic microbial mat communities thrive (Biddanda et al., 2009). Low-oxygen, high-sulfate, brackish groundwater seeps into sinkholes in Lake Huron near Alpena, MI (Ruberg et al., 2005, 2008), which contain lush microbial mats of filamentous cyanobacteria and sulfur-oxidizing bacteria (Biddanda et al., 2006; Nold, Pangborn, et al., 2010; Ruberg et al., 2008). In the 23-m-deep Middle Island Sinkhole (MIS, Figure 1), the sulfidic, anoxic conditions and low-level irradiance (~5%) support a metabolically flexible cyanobacterial mat community dominated by relatives of *Phormidium autumnale* and members of the genus *Planktothrix* (Nold, Pangborn, et al., 2010; Voorhies et al., 2012).

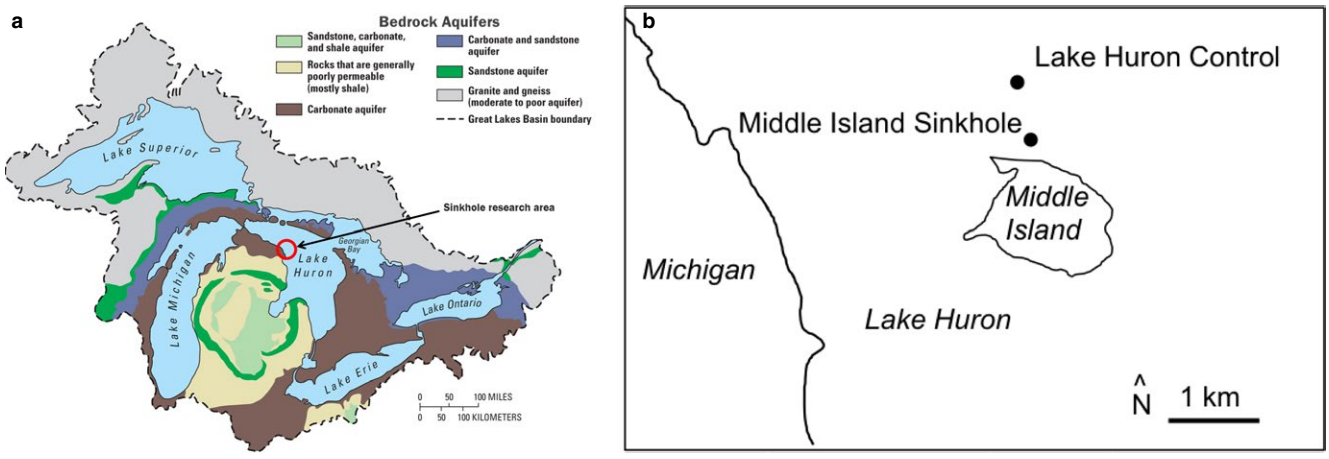

FIGURE 1 (a) Map depicting location of submerged sinkhole research area in Lake Huron and geologic map of bedrock aquifers (modified from Ruberg et al., 2008; Biddanda et al., 2009), (b) map illustrating Middle Island Sinkhole sampling location and nearby Lake Huron "control" site of similar depth and substrate (Map data: Google, NOAA, 2015 TerraMetrics)

As a whole, the MIS mat community is capable of high rates of primary production by a combination of oxygenic photosynthesis, anoxygenic photosynthesis, and chemosynthetic sulfide oxidation (Voorhies et al., 2012). Beneath the cyanobacterial mat, the sinkhole is filled with organic-rich sediment (Nold et al., 2013) that supports a diverse microbial community (Nold, Zajack, & Biddanda, 2010; Nold et al., 2010). Preliminary research by Nold, Pangborn, et al., (2010) and Nold, Zajack, et al., (2010) indicated SO_4^{2-} reduction and methanogenesis in MIS sediments, as well as diverse and active benthic bacterial sediment communities. However, our understanding of this benthic diversity remains limited by the shallow sediment depth sampled (2 cm) and by the number of taxa detected using clone library techniques. For example, none of the clones retrieved were related to known SO_4^{2-}-reducing bacteria (Nold, Pangborn, et al., (2010)), despite the known importance of SO_4^{2-} reduction in the system. To explore the role of underlying sediments in MIS benthic ecosystem functioning and assess vertical stratification of sediment community structure and function more broadly, we sampled sediment cores (0–12 cm) from within the MIS and from a similar depth and substrate texture in a nearby non-sinkhole area of Lake Huron (LH, Figure 1). We find that sinkhole sediment microbial communities are diverse and change with depth through the sediment–water interface and into deep sediments along geochemical gradients that both reflect and shape microbial community function.

2 | METHODS

2.1 | Site description

The MIS (45° 11.914 N, 83° 19.671 W) consists of an approximately 1-hectare sinkhole and groundwater seep at 23 m depth in LH near Alpena, MI (Figure 1; Ruberg et al., 2008). Brackish (specific conductivity = 2300 μs/cm) groundwater carrying salts dissolved from water–rock reactions between groundwater and ~400-million-year-old Detroit River Group (Middle Devonian) limestones and evaporites (Ruberg et al., 2008) flows from an adjacent seep (the "alcove") and spills into the MIS. Seeping groundwater forms an approximately meter-thick "lens" of higher density water above the sediment–water interface that resists mixing with the surrounding fresh LH water (200 μs/cm), establishing a distinct ecosystem bounded by this chemocline (Ruberg et al., 2008). Although irradiance conditions change seasonally at this latitude, other physicochemical characteristics are relatively consistent in the MIS groundwater layer. Specific conductivity, dissolved oxygen, pH, and temperature are relatively stable at 1700 μs/cm, 2–4 mg/L, 7–7.5, and 9.5–12°C, respectively (Ruberg et al., 2008). In comparison, these conditions vary seasonally in overlying Lake Huron water as would be expected in a large freshwater lake (Ruberg et al., 2008, unpublished data).

2.2 | Sediment sample collection and processing

Scuba divers collected sediment cores from the MIS on five dates in June 2011, September 2011, September 2012, May 2013, and July 2013. Microbial community composition and geochemical characteristics were measured in vertically stratified samples from cores collected on all dates. Pore water was also sampled and geochemically characterized from cores sampled in September 2012, May 2013, and July 2013. In May 2013, divers also collected sediment cores from a non-sinkhole location nearby in LH (45° 12.333 N, 83° 19.850 W) of comparable water depth for simultaneous measurement of microbial community composition, sediment geochemistry, and pore water geochemistry. Divers inserted 20 × 7 cm (length × inner diameter) clear polycarbonate tubes through surface mat material and into soft sediments to obtain an intact core preserving the vertical structure of benthic overlying water, mat, and 12–15 cm of sediment.

Cores collected in June and September 2011 were frozen within 24 hr of collection and later divided by sawing into vertical sections (water chemistry was not measured for the frozen samples). Cores collected in September 2012, May 2013, and July 2013 were transported upright and on ice in the dark to Ann Arbor, MI, where they were stored at 4°C in the dark for up to 48 hr. For each of these three sampling events, four replicate cores were sampled and processed by first removing overlying water, then removing surface mat material, and finally dividing each core into vertical sections (3 cm). In September 2012, pore water was sampled from pre-drilled holes using an 18-gauge needle and filtered through 0.45 μm filters (PVDF, Thermo Scientific). In May and July 2013, pore water was sampled from pre-drilled holes at the vertical midpoint of 3-cm sections using soil moisture samplers (Rhizon, Rhizosphere Research Products) with a nominal pore size of 0.2 μm. Pore waters were extracted using syringes attached to Rhizon samplers with three-way valves, creating a closed system that prevented loss of methane gas during sampling. All pore water samples were analyzed for nutrients, major ions, and methane gas. Replicate cores were extruded vertically from the polycarbonate tube and sectioned at 3 ± 0.5-cm intervals for geochemical characterization of sediments. In July 2013, three additional cores were processed such that the top 3 cm of sediment was sectioned vertically into three 1-cm aliquots to be subsampled for microbial community composition and sediment geochemistry. Pore water was sampled at 3-cm intervals, as above. When necessary for statistical analyses, the pore water value measured for the top (0–3 cm) sediment section was related to the solid-phase geochemical measurement or microbial community composition of each of the top three 1-cm segments. Due to limited solid material, mat material was sometimes pooled across replicate cores within season for geochemical characterization.

In September 2012, benthic overlying water chemistry was assessed in surface water siphoned from cores. We observed minimal variability among replicate cores (e.g., across six cores Cl^- concentrations ranged from 21 to 31 mg/L and averaged 27 mg/L, with a standard deviation of 3.8 mg/L). On future sampling dates, benthic overlying water samples were collected by divers using a syringe to obtain water as close to the mat–water interface as possible without causing disturbance. In July 2013, divers collected water venting directly from the adjacent groundwater seep for water chemistry analysis. We measured sediment bulk density in sediment samples taken in May and July 2013.

2.3 | Microsensor measurements

Hydrogen sulfide (H_2S) and oxygen (O_2) concentrations were measured at fine vertical resolution using microsensors in intact cores from the MIS collected in September 2011 and July 2013 within 12 hr of collection. Cores were stored upright on ice in a dark cooler between collection and microsensor profiling at room temperature under ambient indoor light. Amperometric microsensors for O_2 and H_2S (Unisense, 100 μm tip size; Revsbech, 1989; Jeroschewski, Steuckart, & Kühl, 1996) were calibrated according to manufacturer's instructions immediately before profiling. Briefly, the O_2 microelectrode was calibrated with a two-point curve that included air-saturated water and an anoxic solution of 0.1 M sodium ascorbate (in 0.1 M NaOH). The H_2S microelectrode was calibrated with a linear standard curve that covered a H_2S concentration range of 0–5 mM (Na_2S in pH 4 buffer). After each profile, the calibration of the microsensors was verified with a calibration standard and a new curve was prepared if necessary (required for H_2S only). Simultaneous profiling of O_2 and H_2S in cores was carried out using a micromanipulator (Unisense) after aligning the two sensor tips horizontally at the surface of the water in the core. Starting in the overlying water above the mat and sediment, O_2 and H_2S were measured at 500-μm vertical intervals through the mat–water interface until the sensor tip was 2–3 cm into the sediment (Kühl & Revsbech, 2001). Within each core, we completed two to four replicate profiles, each in a different location on the surface of the core. Because pH was not measured concurrently, the data presented here are only the H_2S fraction of total sulfide.

2.4 | Chemical analyses

Cation (NH_4^+, Ca^{2+}, Mg^{2+} and Na^+) and major anion (SO_4^{2-}, NO_3^-, Cl^-) concentrations were quantified using membrane-suppression ion chromatography (Dionex, Thermo Scientific), soluble reactive phosphate (PO_4^{3-}) concentrations using the molybdate blue colorimetric method (Murphy & Riley, 1962), and dissolved methane concentrations using gas chromatography with a flame ionization detector (Hewlett Packard, Tekmar). Total manganese (Mn), iron (Fe), and phosphorus (P) were extracted using microwave assisted digestion (MARS) with a mixture of nitric and hydrochloric acid and quantified with inductively coupled plasma optical emission spectroscopy (PerkinElmer Optima 8000). Sediment organic matter content was quantified in two ways: 1) loss on ignition (LOI) and 2) measuring total organic C and N content using samples decarbonated in weak (2%) HCl, dried, and weighed (~5 mg) into solvent-rinsed tin capsules and then combusted in a Costech ECS4010 elemental analyzer. External precision was maintained at better than 0.1% for both C and N, and results were calibrated against a certified acetanilide standard (C = 71.09%, *N* = 10.36%).

Acid volatile sulfides (AVS) in sediments were quantified using the US EPA Method 821-R-91-100 (Allen, Fu, Boothman, DiToro, & Mahoney, 1991). Briefly, frozen sediment subsamples were acidified (1 M HCl) and released sulfide was captured in an alkaline solution (0.5 M NaOH). Total AVS was quantified colorimetrically with a mixed diamine reagent (H_2SO_4, N,N-dimethyl-p-phenylenediamine oxalate, and ferric chloride hexahydrate). Analytical sulfide standards were prepared from a stock solution (prepared and kept anaerobic under a headspace of N_2 gas) and standardized against a thiosulfate stock solution.

2.5 | Microbial community composition methods

2.5.1 | DNA extraction, quantification, amplification, and Illumina amplicon sequencing

Bulk DNA was extracted from 0.5-g (wet weight) sediment using the FastDNA Spin kit for soil (MP Biomedical, Santa Anna, CA, USA) following the manufacturer's protocol with the exception of using 0.3 g of beads. Total extracted DNA was quantified with PicoGreen (Invitrogen, Carlsbad, CA, USA). 16S rRNA genes were PCR amplified with primers (515F-806R) (Bates et al., 2011) that contained dual index barcodes and Illumina MiSeq specific adapters (Kozich, Westcott, Baxter, Highlander, & Schloss, 2013). PCRs consisted of 10 μ of HotMasterMix (5prime, Gaithersburg, MD, USA), 12 μ(of PCR grade water (Ambion, Life Technologies, Grand Island, NY, USA), 1 μ each of forward and reverse primer (10 SA), 1 A), μe of DNA. Reaction conditions were 94°C for 4 min followed by 30 rounds of 94°C for 30 sec, 50°C for 45 sec, 72°C for 1 min, and a final extension step of 72°C for 10 min. For each sample, triplicate 25-μo PCRs were carried out then pooled prior to cleaning. Pooled PCR samples were cleaned using the UltraClean PCR cleanup kit (MoBio, Carlsbad, CA, USA). Pooled PCRs were quantified with Picogreen (Invitrogen), combined into a single sample at near equivalent concentrations and sent for 2 × 250 sequencing with the Illumina MiSeq platform at the University of Michigan's Microbial Systems Core Sequencing facility. Sequences may be obtained from NCBI Sequence Read Archive (SRA-SRP067517).

2.5.2 | OTU clustering, data analysis, and statistics

Operational taxonomic units (OTUs) were clustered using a modified Uparse pipeline (Edgar, 2013). With Uparse, Illumina paired sequence reads (iTags) were joined (flags: –fastq_mergepairs) and filtered and length truncated (flags: -fastq_filter, -fastq_maxee 1.0, and –fastq_trunclen 250). iTags were dereplicated with an in-house perl script (available at github.com/Geo-omics/scripts), sorted, and then, OTUs were clustered at a 0.97 cutoff. OTUs were classified to the Silva v.111 taxonomy (Pruesse et al., 2007) with the naive Bayesian classifier (Wang, Garrity, Tiedje, & Cole, 2007) in Mothur (v 1.31) (Schloss et al., 2009). A phylogenetic tree of representative OTU sequences (with chloroplasts and mitochondria omitted) was calculated with FastTree (Price, Dehal, & Arkin, 2009). Using the R statistical environment (R Core Team 2015), an OTU table was rarefied to a uniform depth (13,000 iTags per sample) and phylogenetic diversity (PD) (Faith, 1992) was calculated with Picante (Kembel et al., 2010). Prior to ordination calculation, the OTU abundances were normalized

with DESeq (Anders & Huber, 2010), as suggested by McMurdie and Holmes (2014). Non-metric multidimensional scaling (NMDS) plots were calculated with Bray–Curtis dissimilarities using the metaMDS function (autotransformation=F, binary=F).

We used ANOSIM to test for significant differences in OTU community composition between LH sediment, MIS mat, and MIS sediment (Clarke, 1993). To test for differences between MIS and LH and for changes in parameters along vertical gradients, we used linear mixed-effects models. The models use an ANCOVA design, predicting response variables (geochemical parameters or microbial relative abundance data at different taxonomic levels) from the fixed effects of location (categorical), depth into sediments (continuous), and the interaction between them. Random effects of sample date and intact core identity were included in these mixed-effects models to account for variability associated with these factors.

To assess relationships between sediment microbial community composition and geochemical characteristics, we conducted Mantel tests comparing dissimilarity matrices based on normalized prokaryotic OTU reads (Bray–Curtis distance) and sediment pore water and geochemical characteristics (Euclidean distance). We first compared community composition to the entire suite of geochemical characteristics to assess the overall relationship between sediment geochemistry and microbial community composition in each of the two locations, MIS and LH. Due to incomplete data across samples, sediment LOI and AVS were omitted from these "whole-suite" analyses, and pore water CH_4 was omitted from the LH analysis. After omitting sediment samples with incomplete geochemical data, 11 and 34 samples from LH and MIS were tested, respectively. We also used Mantel tests to assess relationships between microbial community composition differences and differences among individual geochemical variables. Within all groups of results, significance values (α = .05) were corrected for multiple comparisons (Benjamini & Hochberg, 1995). Unless stated otherwise, values are stated as means ± standard deviation.

3 | RESULTS

3.1 | Solid-phase sediment geochemistry

Geochemically, sediments from MIS and LH demonstrated many qualitative and quantitative differences (Table 1). Sediments from MIS were darker, finer, and less dense than the sandier LH sediments. MIS sediments contained significantly more organic matter than LH sediments, when measured as total organic C, total organic N, and LOI (Tables 1 and 2). In both MIS and LH sediments, organic C and N decreased with depth and C:N ratio increased with depth (Table 2). Low organic N led to high C:N ratios in LH sediments (Table 2).

Sediment total Fe, total Mn, and total P concentrations were generally higher in MIS sediments than LH sediments (Table 1). In MIS, total Fe increased significantly with depth into sediments (Tables 1 and 2). In contrast, total Fe decreased with depth in LH sediments (Tables 1 and 2). Sediment total P significantly decreased with depth in both MIS and LH sediments (Tables 1 and 2). Phosphorus was more concentrated in the surface mat material than sediments below (Table 1). In MIS sediments, AVS did not change significantly with depth, although concentrations were more variable in surface sediments than in deeper sediments (Table 1). Averaged across depths, MIS AVS concentrations (67 ± 25 μmol S/g n = 23) were an order of magnitude higher than AVS concentrations in LH sediments (6.4 ± 3.5 μmol S/g; n = 3).

3.2 | Benthic and pore water geochemistry

Biologically reactive solutes (SO_4^{2-}, NH_4^+, PO_4^{3-}, and CH_4) displayed steep vertical gradients in MIS sediments, and also changed with depth in LH sediments, but at lower concentrations (Figure 2, Table 2). In contrast, more conservative ions (Ca^{+2}, Mg^{+2}, Na^+, and Cl^-), which are indicators of groundwater influence, did not change significantly with depth in MIS sediments, but increased with depth in LH sediment cores, reflecting likely subsurface groundwater influence. Ammonium

TABLE 1 Solid-phase characteristics of sediments collected from the Middle Island Sinkhole (MIS Sed) and a nearby non-sinkhole location in Lake Huron (LH Sed) of similar depth and cyanobacterial mat material from the sinkhole (MIS Mat). Data are from cores collected in September 2012 (MIS), May 2013 (MIS and LH), and July 2013 (MIS). Values are means plus or minus standard deviation

Location	Depth (cm)	n^a	Bulk density (g/cm^3)	Loss on ignition (%)	Organic C (%)	Organic N (%)	Molar C:N	Total Mn (μmol/g)	Total Fe (μmol/g)	Total P (μmol/g)	AVS (μmol/g)
MIS Mat		4	nm	28.4 ± 7.9^d	11.3 ± 0.8^e	1.6 ± 0.1^e	8.2 ± 0.1	2.9 ± 0.5	164 ± 33	92 ± 39	nm
MIS Sed	1.9 ± 0.2	12	0.2 ± 0.08^b	10.7 ± 4.7	8.6 ± 2.7	1.1 ± 0.4	8.9 ± 0.4	3.6 ± 0.7	235 ± 11	31 ± .5.8	85 ± 48^f
	5 ± 0.1	12	0.26 ± 0.10^b	7.4 ± 1.9	6.4 ± 1.5	0.8 ± 0.2	9.5 ± 0.5	4.3 ± 1.0	224 ± 29	24 ± 4.1	58 ± 19^f
	8 ± 0.2	11	0.26 ± 0.05^b	7.9 ± 1.5	6.4 ± 0.9	0.8 ± 0.1	9.4 ± 0.3	4.5 ± 0.8	255 ± 15	23 ± 2.5	64 ± 23^f
	11.2 ± 0.3	11	0.38 ± 0.14^c	7.7 ± 1.4	6.2 ± 0.9	0.8 ± 0.1	9.5 ± 0.5	4.5 ± 0.9	271 ± 16	22 ± 2.2	60 ± 7^f
LH Sed	1.5 ± 0	4	0.8 ± 0.44	3.0 ± 0.2	2.1 ± 0.3	0.3 ± 0.02	10.1 ± 0.4	3.8 ± 1.1	175 ± 30	16 ± 2.3	8^g
	4.5 ± 0.1	4	0.88 ± 0.14	1.7 ± 0.2	1.0 ± 0.2	0.1 ± 0.01	12.4 ± 1.8	2.8 ± 0.6	157 ± 27	14 ± 3.1	9^g
	6.9 ± 0.2	4	0.52 ± 0.21	1.8 ± 1.4	0.6 ± 0.1	0.1 ± 0.02	13.8 ± 1.5	2.0 ± 0.4	123 ± 25	11 ± 1.6	2^g

nm = not measured.
[a]Sample size (number of replicate cores), unless otherwise noted.
[b]n=8; [c]n=7; [d]n=5, [e]n=7, [f]n=3, [g]n=1.

TABLE 2 Results (*p* values) of mixed-effects models (except where noted) testing the effects of location (Middle Island Sinkhole, MIS, vs. Lake Huron, LH) and depth into sediments (MIS Slope, LH Slope) on geochemical characteristics, accounting for the random effects of sample date and intact core (not shown). Significant ($p < .05$, after Benjamini and Hochberg (1995) correction) terms are in bold. Detailed statistical results are shown in supplemental materials (Table S2). For significant slopes, the sign of the relationship is indicated in parentheses, with (+) indicating that the parameter increases with depth into sediments and (−) indicating decreases with depth into sediments

	df[b]	MIS slope	MIS vs. LH	LH slope
Pore water chemistry				
SO_4^{2-}	54	**<0.001 (−)**	**0.002**	**<0.001 (+)**
NH_4^+	54	**<0.001 (+)**	**<0.001**	0.915
NO_3^-	57	0.064	**<0.001**	**0.007** (−)
SRP	55	**<0.001 (+)**	**<0.001**	0.405
CH_4	46	**<0.001 (+)**	**<0.001**	0.067
Ca^{2+}	54	0.956	**<0.001**	**<0.001 (+)**
Mg^{2+}	54	**0.020 (+)**	**<0.001**	**<0.001 (+)**
Na^+	53	0.667	**<0.001**	**<0.001 (+)**
Cl^-	54	0.140	**0.031**	**<0.001 (+)**
Sediment geochemistry				
Loss on ignition	35	**0.001**	**0.001**	0.765
Organic C	50	**<0.001** (−)	**<0.001**	**<0.001** (−)
Organic N	50	**<0.001 (−)**	**<0.001**	**<0.001** (−)
C:N molar ratio	50	**<0.001 (+)**	0.41	**<0.001 (+)**
Total Mn	44	**<0.001 (+)**	0.395	**<0.001** (−)
Total Fe	44	**0.002 (+)**	0.178	**<0.001** (−)
Total P	44	**<0.001** (−)	**<0.001**	0.432
AVS[a]	11	0.569	0.026	0.151

[a]Acid volatile sulfide, linear model testing the fixed effects of depth and location on the response variable (measured in both MIS and LH, but not on multiple TimeIDs).
[b]Residual degrees of freedom.

and PO_4^{3-} both increased significantly with depth into MIS sediments to much higher concentrations than in deep LH sediments (Figure 2, Table 2). Pore water NO_3^- concentrations in MIS were uniformly low (1.5 ± 1.5 μM) and did not change significantly with depth into sediments (Table 2, Figure 2). In contrast, LH benthic waters contained measureable concentrations of NO_3^- (20 ± 2.5 μM), which decreased significantly with depth (Table 2, Figure 2) to 1.2 ± 0.1 μM. The source groundwater seeping into the MIS from the "alcove" contained low-nutrient concentrations: 13 μM NO_3^-, 9 μM NH_4^+, and 1 μM PO_4^{3-}(Ruberg et al., 2008).

Sulfate concentrations in benthic water overlying MIS mats were 7.1 ± 1.5 mM, much higher than in LH (0.2 ± 0.04 mM), reflecting input from the MIS groundwater seep (11 mM SO_4^{2-}, Figure 2). Sulfate concentrations significantly decreased with depth into MIS sediments, from 4.5 ± 2.2 mM in the top 0–3 cm of sediments to 0.5 ± 0.5 mM in the bottom 9–12 cm of sediments (Figure 2, Table 2). Conversely, SO_4^{2-} concentrations in LH sediments increased with depth, 0.8 ± 0.5 in the top 0–3 cm to 5.4 ± 0.8 mM in the bottom 6–9 cm (Figure 2, Table 2).

Microsensor measurements of intact MIS sediment cores revealed that O_2 concentrations decrease to below detection within 1–3 cm into the sediments (Figure 3). Hydrogen sulfide was detected within the surface mat, and increased with depth to high concentrations of 1–7 mM within the top 0–3 cm of sediments and, in some profiles, showed no evidence of leveling off at this depth (Figure 3). Hydrogen sulfide concentrations in pore waters vary considerably across space and season (Figure 3). The apparent co-occurrence of H_2S and O_2 in some profiles is likely due to artifacts either from a "hole effect" produced by the relatively deep profiles and/or rapid sensor measurements that were not allowed to equilibrate to accurate measurements. However, the general patterns of O_2 depletion and H_2S increase with depth illustrated by these data are robust, and measurement artifacts do not invalidate the conclusion that the mats represent net sinks of O_2 and net sources of sulfide. In fact, our measurements likely underestimate O_2 and H_2S fluxes. In addition, although we did not measure pH and thus sulfide concentrations are presented as only the H_2S fraction of total hydrogen sulfide, the general patterns are unlikely to change with pH correction.

Methane concentrations in sediment pore waters and overlying benthic waters were higher in MIS than LH sediments (Figure 2). In MIS sediment pore waters, CH_4 concentrations increased significantly with depth (Figure 2, Table 2), but there was considerable temporal variability. Methane concentrations were the highest in July and September (63–2030 μM range) and lowest in May (37–223 μM range). Across seasons, MIS CH_4 concentrations tended to be highest at mid-depths (3–6 cm; 521 ± 603 μM), with slightly lower concentrations in deeper and shallower sediments (0–3 cm: 183 ± 147 μM; 6–9 cm: 321 ± 314 μM; 9–12 cm: 395 ± 273 μM). Concentrations of CH_4 in deep LH sediments were much lower (2.5 ± 0.3 μM).

3.3 | Microbial community composition

We detected 14,127 unique microbial operational taxonomic units (OTUs) across 114 total samples. Over a third of all OTUs (5,290) were detected in every sample type: MIS mats, MIS sediments, and LH sediment (Figure S1). Only 103 OTUs were unique to MIS mats, and these were all detected at low abundance (<122 reads). Most high-abundance OTUs were either shared among all three groups or were shared between MIS mats and MIS sediments but absent from LH sediments (Figure S1–S2). Of the OTUs detected, 174 were classified as mitochondria or chloroplasts. Whole-community composition patterns were similar whether OTUs classified as chloroplasts and mitochondria were included or omitted from the analysis (Figure S3). We detected OTUs representing 53 phyla of *Bacteria*. More *Archaea* were detected in sediments than in MIS surface mats, and all archaeal OTUs detected were classified as belonging to the phylum *Euryarchaeota* (Figure 4).

Despite the large number of shared OTUs, the structure of microbial communities in MIS sediment and mat samples was distinctly different from that in LH sediments (ANOSIM, $R = .73$, $p = .001$, Figure 5). MIS microbial mats were dominated by *Cyanobacteria*, whereas underlying

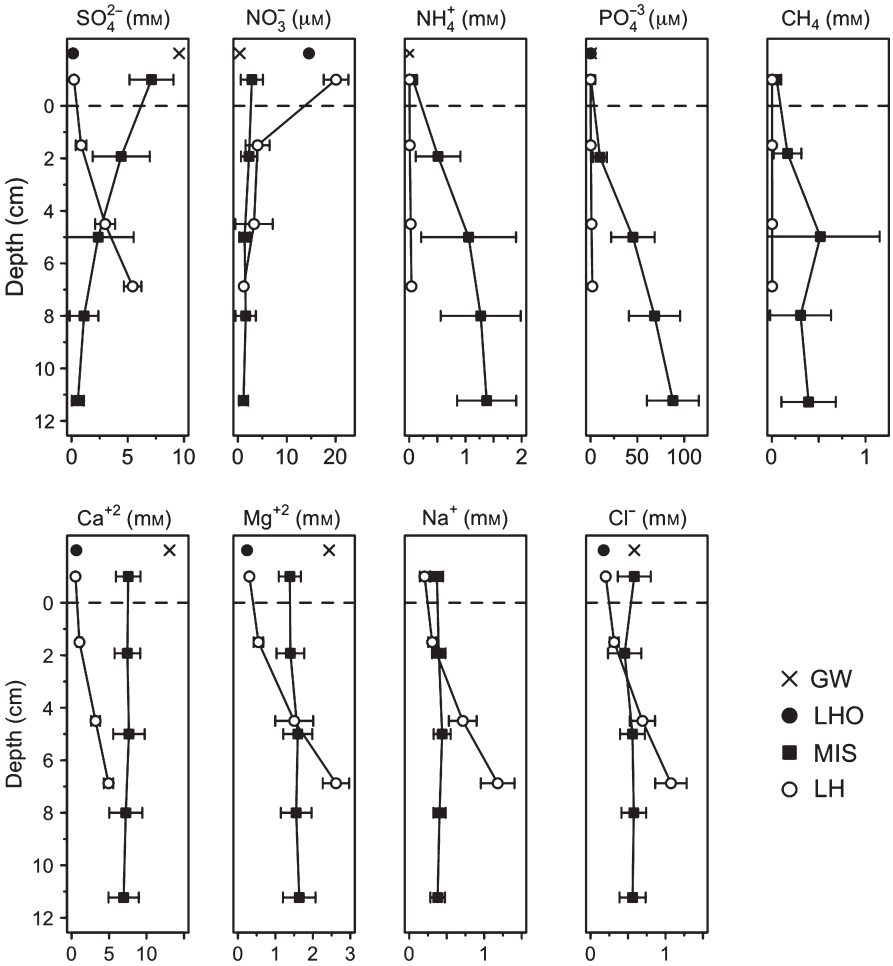

FIGURE 2 Mean concentrations (± 1 standard deviation) of dissolved solutes in overlying benthic and sediment pore water in the Middle Island Sinkhole (MIS), nearby Lake Huron sediments (LH), compared with concentrations in groundwater at the "alcove," the major seep feeding the MIS (GW) and overlying surface Lake Huron water (LHO). The dashed line indicates the sediment–water interface, with positive depth values denoting vertical distance below the sediment–water interface. MIS values represent means of pore water concentrations measured in four replicate cores on each of September 2012, May 2013, and July 2013 (n = 16), whereas LH values represent means of four replicate cores sampled only in May 2013

MIS sediments were dominated by *Bacteriodetes* and *Proteobacteria* (Table S1, Figure 4). Lake Huron sediments had fewer *Bacteriodetes* and more *Nitrospirae* than MIS sediments (Figure 4). LH sediment communities displayed less variability among LH samples than among MIS samples (Figure 5). MIS mat communities overlapped somewhat with MIS sediment communities (Figure 5). Microbial community composition changed with depth into sediments in both MIS and LH (Figure 5). In MIS, 18 of the 19 major microbial groups changed significantly with depth (p < .05), whereas only six of the 19 changed significantly with depth in LH sediment cores (Figure 6).

3.3.1 | Cyanobacterial mat community

Ninety-five of the 380 OTUs classified as *Cyanobacteria* were chloroplasts, including several of the high relative abundance OTUs. The most abundant of these (OTU_2) was classified as a relative of the diatom *Odontella sinensis*, but with only 22% maximum likelihood. Other OTUs identified as chloroplasts were similar to sequences without meaningful taxonomic information. The four non-chloroplast *Cyanobacteria* OTUs with high average relative abundance (>1%) in the MIS surface mat samples were representatives of the genera *Phormidium* (OTU_1, OTU_3202) and *Planktothrix* (OTU_7, OTU_2819). The two high-abundance *Phormidium* OTUs, OTU 1 and OTU 3202, were 100% and 98% similar, respectively, in sequence to a dominant *Phormidium* previously detected in MIS mats (Voorhies et al., 2012). Although *Plantktothrix* (formerly called *Oscillatoria*) has traditionally been found in pelagic environments, it has been found both in MIS mats and cyanobacterial mat communities in other sulfidic environments (Klatt, Haas, Yllmaz, de Beer, & Polerecky, 2015; Camacho, Vicente, & Miracle, 2000; Voorhies et al., 2012). In LH sediments, the only OTUs classified as *Cyanobacteria* with meaningful relative abundances were chloroplasts. Mat communities and surface sediments contained other evidence of eukaryotes in abundant mitochondria (e.g., OTU_28) and an amoeba symbiont (OTU_107).

3.3.2 | Putative sulfate-reducing bacteria

We detected OTUs classified to five orders containing known SO_4^{2-}-reducing bacteria (SRB): *Desulfarculales*, *Desulfobacterales*, *Desulfovibrionales*, *Desulfurellales*, and *Desulfuromonadales*. All high relative abundance putative SRB were phylogenetically related to members of the *Desulfobacterales*. Two putative SRB, OTU_3 and OTU_9, were among the most abundant non-*Cyanobacteria* OTUs across all samples. The most abundant putative SRB in the surface mats, OTU_3, was phylogenetically classified (maximum likelihood=100) as genus *Desulfonema* a filamentous SO_4^{2-} reducer that was also detected in the Frasassi cave system (ACC No. DQ133916, Macalady et al., 2006). Relative abundances of this OTU decreased with depth (Figure 7) in

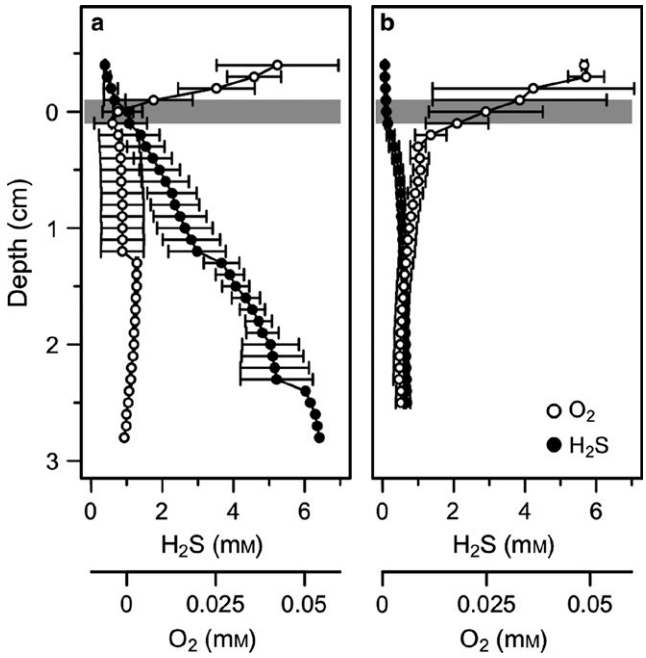

FIGURE 3 Microelectrode measured vertical profiles of dissolved oxygen (O_2, open circles) and hydrogen sulfide (H_2S, filled circles) in representative intact cores sampled from the Middle Island Sinkhole in September 2011 (a) and July 2013 (b). The gray rectangle indicates the approximate location of the sediment–water interface, with positive depth values denoting vertical distance below the sediment–water interface. Points represent averages of two to four replicate profiles with standard deviation bars. Elevated oxygen concentrations above the sediment–water interface may be laboratory artifacts due to oxygen diffusion through overlying water during core handling and processing

the MIS and were very low in LH sediments. The other high-abundance OTU (OTU_9) was classified as a member of the genus *Desulfocapsa* and also showed highest abundance in mats with decreasing abundance with depth into MIS sediments (Figure 7) and very low abundance in LH sediments. *Desulfocapsa* can disproportionate elemental sulfur and thiosulfate (Finster, Liesack, & Thamdrup, 1998).

In contrast to these putative SRB OTUs with highest relative abundance in MIS surface mats, several putative SRB increased with depth into MIS sediments (Figure 7). An OTU classified to the genus *Desulfatirhabdium* (OTU_13) was the most abundant putative SRB in sediments beneath the MIS surface mat. The only named species in this genus oxidizes butyrate and reduces sulfur (Balk, Altinbaş, Rijpstra, Damsté, & Stams, 2008). The most abundant putative SRB in LH sediments (OTU_41) was classified to the genus of the SVa0081 sediment group. This OTU was also detected at lower abundances in MIS sediments and mats (0.15% and 0.04%, respectively) and did not change with depth in MIS or LH.

3.3.3 | Putative sulfur oxidizers

Relative abundances of putative sulfide oxidizers of the *Epsilonprotoeobacteria* and *Beggiatoa* sp. relatives were higher in MIS communities than in LH sediments (Figure 4, Table S1). Similar to the putative SRBs, putative sulfide-oxidizing OTUs showed variable vertical patterns with depth into sediments. OTUs related to *Sulfurospirillum* (OTU_19), *Helicobacteraceae* (OTU_33), and *Beggiatoa* (OTU_4) were detected at highest relative abundance in surface mat material and decreased with depth into sediments (Figure S4). In contrast, relatives of *Sulfuricurvum* (OTU_14192 and OTU_22), and another *Sulfurospirillum* (OTU_18), had higher relative abundance in underlying MIS sediments, with some evidence for a peak at intermediate depths (3–6 cm; Figure S4).

3.3.4 | Euryarchaeota

All *Euryarchaeota* taxa tended to increase in relative abundance with depth into the sediments. Of the 1248 OTUs classified in the Phylum *Euryarchaeota*, only 21 were identified as putative methanogens (18 OTUs in the *Methanomicrobia*, 3 OTUs in the *Methanobacteria*). Putative methanogens were highest in abundance in deep MIS sediments, detected at much lower relative abundance in LH sediments, and exceedingly low in abundance or not detected in MIS surface mats. Two putative methanogens, OTU_117 and OTU_252, of the genus *Methanosaeta* and *Methanoregula*, respectively, dominated the methanogenic community of MIS sediments.

Other high-abundance sediment *Euryarchaeota* OTUs were related to *Halobacteria* and *Thermoplasmota*. Of the four classes to which *Euryarchaeota* OTUs were classified, deep-sea hydrothermal vent *Halobacteria* (1145 OTUs) represented the highest relative abundance in sediments, followed by *Thermoplasmata* (82 OTUs). Most archaeal OTUs were associated with members of the uncultured *Woesearchaeota* (formerly DHVEG-6). Two *Woesearchaeota* OTUs, OTU_84 and OTU_85, were among the highest abundance archaeal OTUs and showed nearly identical patterns within cores, increasing with depth in MIS sediments, and virtually undetected in LH sediments and MIS surface mat material.

3.3.5 | Putative methanotrophs

We detected 30 OTUs classified as aerobic *Gammaproteobacteria Methylococcales*, although at low relative abundances (0%–0.34%). *Methylococcales* OTU relative abundances were highest at intermediate sediment depths (2–5 cm) on average. We did not detect any OTUs allied with members of the NC10 phylum (denitrifying methanotrophs), despite the high concentrations of methane detected in pore waters. Only one detected OTU (OTU_11930) had low phylogenetic similarity to known archaeal anaerobes that pair methane oxidization to sulfate reduction (ANME-1). This OTU was detected only in 10 deep (>5 cm) sediment samples at very low relative abundance (0.0003%–0.004%).

3.3.6 | Microbial community composition significantly correlated to geochemical gradients

Differences in microbial community composition among samples were significantly related to their geochemical differences in both MIS

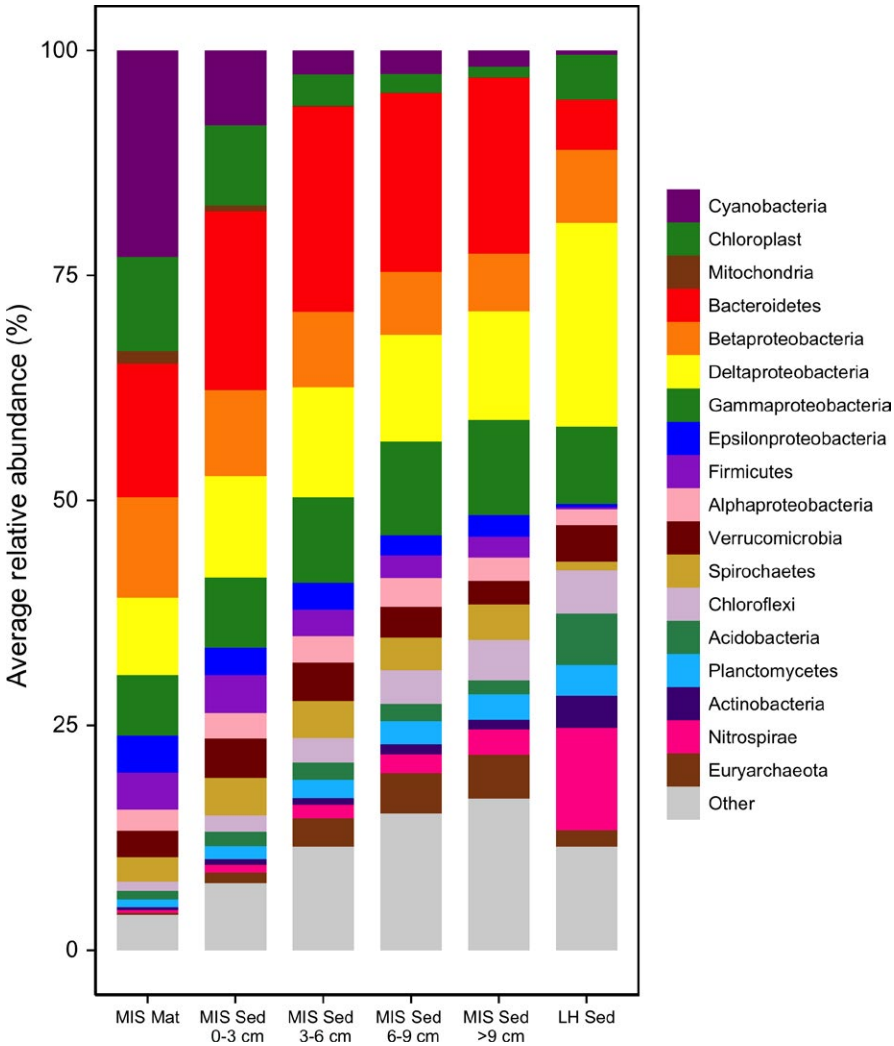

FIGURE 4 Average relative abundance of OTUs categorized into major groups across samples of Middle Island Sinkhole mat material (MIS Mat, n = 17), MIS underlying sediments (MIS Sed, n = 87: 0–3 cm n = 31; 3–6 cm n = 17; 6–9 cm n = 22; >9 cm n = 17), and non-sinkhole Lake Huron sediments (LH Sed, n = 11). Summary relative abundances of major groups in MIS sediment, LH sediment, and MIS mat samples are tabulated in Table S1

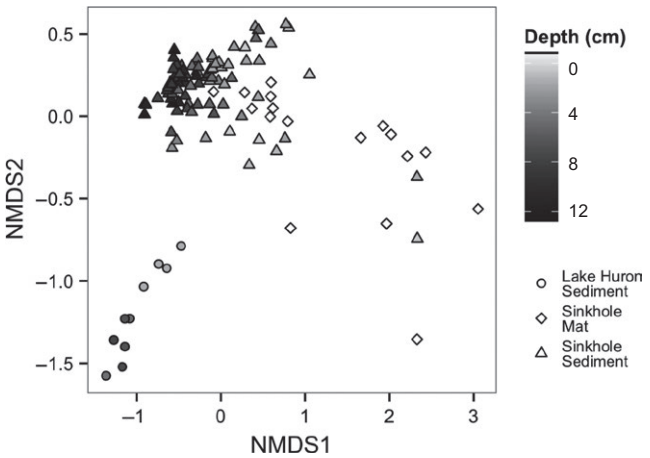

FIGURE 5 Non-metric multidimensional scaling ordination of microbial communities in microbial mat and sediment material collected from the Middle Island Sinkhole (Sinkhole Mat and Sinkhole Sediment, respectively) in Lake Huron, MI, and in sediment material collected in a nearby non-sinkhole area of Lake Huron at comparable depth (Lake Huron Sediment). Points are shaded by depth into the sediment, with 0 representing the sediment–water interface, and higher numbers reflected depth (in cm) below the sediment–water interface

(r_{Mantel} = .5439, p = .001, n = 34) and LH sediments (r_{Mantel} = .7761, p = .002, n = 11). Specifically, MIS community differences were significantly related to differences in multiple indicators of nutrient availability, including pore water PO_4^{3-} and NH_4^+ concentrations, and sediment organic C, organic N, LOI, total Fe, and total P (Table 3). LH sediment community differences were also significantly related to some nutrient availability indices (PO_4^{3-}, NH_4^+, organic C, organic N), but indices of groundwater influence (concentrations of SO_4^{2-}, Cl^-, Na^+, Ca^{2+}, and Mg^{2+}) also strongly predicted community differences (Table 3).

4 | DISCUSSION

Submerged Great Lake sinkholes contain diverse microbial communities shaped by low-oxygen, brackish groundwater (Biddanda et al., 2009; Nold, Pangborn, et al., 2010; Nold, Zajack, et al., 2010) that may provide insights into the microbial ecology and biogeochemistry of ancient ecosystems. By deeply sequencing the microbial community at multiple sediment depths in the MIS in parallel with extensive geochemical characterization of pore

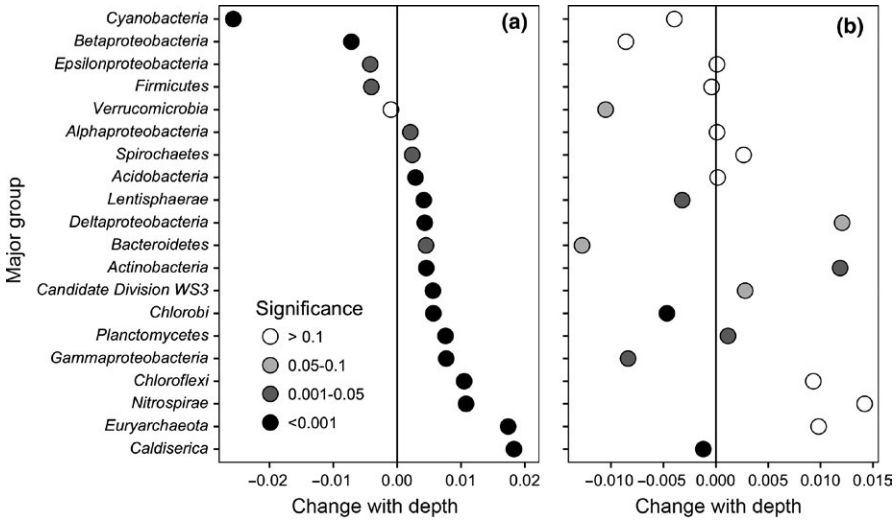

FIGURE 6 Degree of change with depth into sediments of relative abundance of major microbial groups in the Middle Island Sinkhole (a, MIS) and Lake Huron sediments (b, LH). Points to the left of the vertical 0-line represent major groups that decreased with relative abundance with depth into sediments, and points to the right represent groups that increased with depth. Change with depth is the slope of the relationship between arcsine square root-transformed major group relative abundance and depth into sediments (with zero being the sediment–water interface, and surface mats assigned a value of −1 cm) as modeled by a mixed-effects model accounting for the random effects of sampling date and intact core. Significance levels are based on *p*-values corrected for multiple comparisons using the Benjamini and Hochberg correction. Major microbial groups represented at least 1% relative abundance in MIS surface mats, MIS sediments, or LH sediments

water and sediment nutrient concentrations, we have expanded our understanding of this unique ecosystem. The results presented here indicate that the MIS ecosystem is geochemically and biologically distinct from the surrounding freshwater benthic system of Lake Huron and that it is highly vertically stratified through the photosynthetic and chemosynthetic surface mat and into the high-nutrient sediments below, where sulfur and methane cycling become dominant.

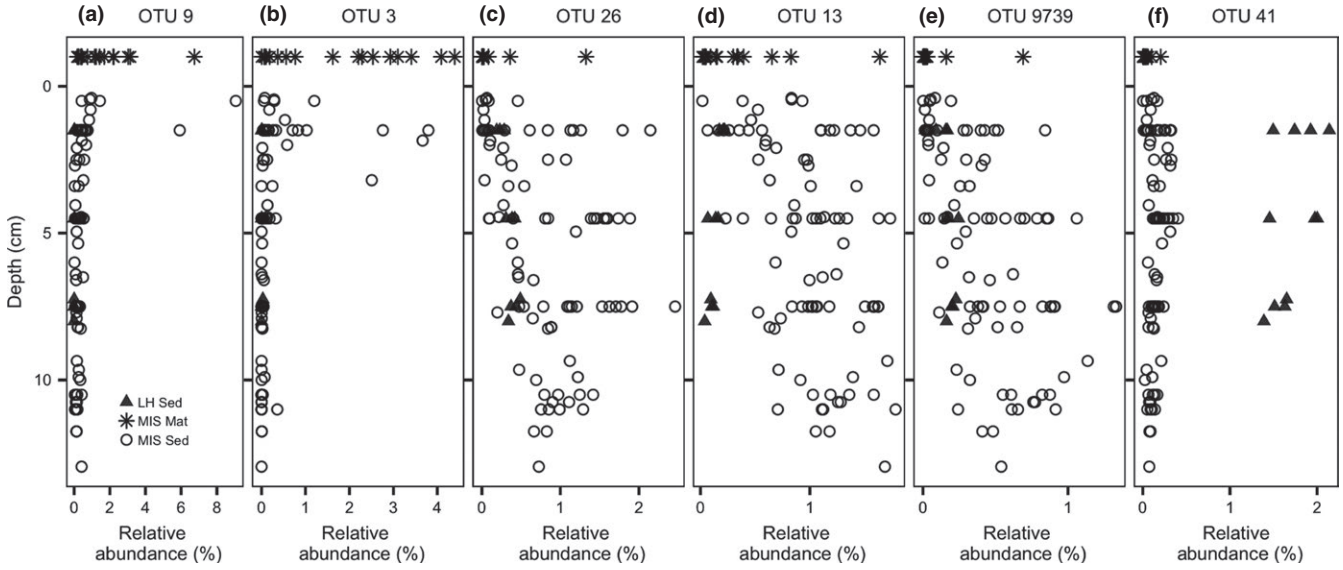

FIGURE 7 Relative abundance of OTUs taxonomically associated with known sulfate-reducing bacteria detected in DNA sequenced from Middle Island Sinkhole surface mat material (MIS Mat) and underlying organic sediments (MIS Sed) in comparison with sandy Lake Huron sediments from comparable depth (LH Sed) plotted versus depth into sediments, with "0" denoting the sediment–water interface. All OTUs are classified as members of the *Deltaproteobacteria*. Based on the finest level of classification with maximum likelihood greater than 90, OTUs are classified as follows: (a) OTU 9, uncultured *Desulfocapsa*; (b) OTU 3, uncultured *Desulfonema* with 100% maximum likelihood classification as a filamentous sulfate reducer also found in limestone-corroding biofilms from the Frasassi caves (AccNo DQ133916, Macalady et al., 2006); (c) OTU 26, uncultured *Desulfobacteraceae*, (d) OTU 13, uncultured *Desulfatirhabdium*, (e) OTU9739, uncultured *Desulfobacteraceae*, (f) OTU 41, uncultured *Desulfobacteraceae* related to a genus of the SVa0081 sediment group (AccNo AB630779)

TABLE 3 Results of Mantel tests, including sample size (*n*), Mantel statistic (r_M), and significance (*p*), of Mantel tests for relationships between microbial community pairwise distances (Bray–Curtis) and geochemical variable pairwise distances (Euclidean) among samples collected from the Middle Island Sinkhole (MIS) and a site of similar depth in Lake Huron (LH). Due to low sample size, the relationship between AVS and LH community composition was not assessed. Relationships with r_M >.5 are in bold

	MIS			LH		
	n	r_M	*p**	*n*	r_M	*p**
Water chemistry						
SRP	58	**.581**	**.002**	11	**.519**	**.038**
NH_4^+	58	**.603**	**.002**	11	**.555**	**.013**
NO_3^-	58	.028	.318	11	.097	.243
SO_4^{2-}	58	.018	.388	11	**.791**	**.002**
Cl^-	58	.148	.049	11	**.762**	**.003**
Na^+	57	.016	.406	11	**.752**	**.003**
Ca^{2+}	58	.029	.309	11	**.684**	**.002**
Mg^{2+}	58	−.003	.486	11	**.777**	**.002**
Sediment chemistry						
Organic C	96	**.548**	**.002**	11	**.582**	**.003**
Organic N	96	**.530**	**.002**	11	**.604**	**.002**
Loss on ignition	42	**.782**	**.002**	7	.209	.130
Total Fe	47	**.520**	**.002**	11	.294	.049
Total P	47	**.766**	**.002**	11	.475	.014
Total Mn	47	.289	.003	11	**.643**	**.002**
AVS	22	.122	.224	NA		

*Corrected for multiple comparisons (Benjamini & Hochberg, 1995).

4.1 | The sinkhole ecosystem is distinct

We compared biogeochemical conditions in the MIS to a reference location in LH of similar depth. Despite evidence of groundwater upwelling at the LH site based on conservative ions (Figure 2), benthic conditions within the MIS and at the LH "control" site are vastly different. In the MIS, groundwater venting out of an adjacent seep that spills and settles into the sinkhole establishes a benthic ecosystem with stable physicochemical conditions (with the exception of light, which changes seasonally) that rarely mixes with overlying freshwater (Ruberg et al., 2008), creating distinct geochemical and ecological conditions at the sediment–water interface. In comparison, despite apparent groundwater influence at LH, the sediment–water interface reflects the chemistry of seasonally variable, low-conductivity LH waters (Sanders, Biddanda, Stricker, & Nold, 2011).

At coarse and fine taxonomic levels, the biotic communities of the MIS and LH sediments differ greatly. Despite the presence of many shared OTU sequences among MIS and LH samples, microbial communities of the MIS sediments are starkly different than communities of LH sediments when considering relative abundances (Figures 5–7). Although deeper LH sediments experience groundwater influence, the microbial community of these sediments was still more similar to that of shallow LH sediments than any MIS sinkhole sample. As expected, we observed vertically stratified microbial communities in sediments from both ecosystems, although it was most pronounced in MIS. Vertical stratification occurs not only at the level of major taxonomic groups, but also at the level of individual OTUs within taxonomic and functional groups (Figures 5–7). Overall, MIS microbial community composition at the OTU level was stratified by relationships with nutrients and redox chemistry, while LH communities were more related to gradients in conservative indicators of groundwater influence (Tables 1 and 2) (although we cannot rule out that these geochemical measurements are indicative of other correlated factors that we did not measure). These differences between sites illustrate the importance of groundwater influence at the sediment–water interface in establishing the unique community of the MIS, both in the microbial mat and in underlying sediments.

4.1.1 | Nutrient-rich sediments

Despite experiencing light conditions that are presumably similar to the MIS, LH sediment cores contained no visible surface microbial mat, and no molecular evidence of *Cyanobacteria* was detected. It seems that the chemical environment established by venting groundwater in the MIS allows microbial mat communities to establish, in part by relieving grazing pressure due to low dissolved oxygen concentrations (Stal, 1995). The MIS microbial mat is capable of high primary production rates (Voorhies et al., 2012), yet underlying sediments largely reflect isotopic characteristics of settling phytoplankton (Nold et al., 2013), implying rapid decomposition of mat biomass prior to burial (Canfield & Des Marais, 1993) and/or significant upward mat motility (Biddanda, McMillan, Long, Snider, & Weinke, 2015) to avoid burial.

Surface microbial mats in the MIS are surrounded by low-nutrient overlying water and thus likely depend on inorganic nutrients diffusing up from pore waters for growth. Concentrations of dissolved nutrients in the MIS pore waters are remarkably higher than in non-sinkhole LH sediments. In addition, MIS sediments contain more solid organic material than typical LH sediments, and the material is of higher nutrient quality (lower C:N ratio). The high-nutrient nature of the MIS sediments is likely due to a combination of abiotic environmental conditions established by venting groundwater and biotic microbial community effects. The low-oxygen environment of the sinkhole likely slows decomposition of settling particles, establishing sediments containing a higher proportion of organic matter than surrounding "typical" Lake Huron sediments.

Although microbial mat biomass is often rapidly, and sometimes completely, decomposed before burial (Canfield & Des Marais, 1993), mats likely play direct and indirect roles in establishing and maintaining high-nutrient conditions of underlying sediment material, further enhancing the high-nutrient conditions encouraged by the low-oxygen environment. The mats may play a direct role in sediment nutrient conditions through their motility, which allows them to physically bury organic particles (Biddanda et al., 2015; Stal, 1995). In addition, their extracellular polysaccharide matrix can slow diffusion of nutrient molecules and limit re-suspension of particles into overlying waters

(Decho, 1990). Mat cyanobacteria may further prevent loss of valuable nutrients to benthic overlying water by sequestering nutrients within their biomass through luxury uptake and storage (Kromkamp, 1987). Molecular evidence reveals that the dominant MIS surface mat cyanobacteria *Phormidium* genome encodes phycobilisome proteins (Voorhies et al., 2016), pigments that can be plentiful in cyanobacteria (Bogorad, 1975) and are degraded by cells experiencing N stress (Luque, Zabulon, Contreras, & Houmard, 2001), implying a role as N storage molecules. In comparison, although LH sediments likely receive comparable nutrient inputs from settling pelagic material, the higher oxygen environment there likely leads to nutrient loss as particles are more rapidly decomposed.

4.1.2 | Sulfur cycling

The influence of high-SO_4^{2-} groundwater in the MIS establishes an ecosystem that contains much more sulfur than typical freshwater ecosystems. Combined with anoxic conditions and abundant organic matter, this provides ideal conditions for microbial SO_4^{2-} reduction, resulting in high concentrations of sulfide, a portion of which is sequestered as AVS by binding with Fe and other metals. Despite high sulfur concentrations in the MIS habitat, microbial community composition was not statistically related to the geochemical indicators of sulfur cycling that we measured (SO_4^{2-}, AVS). Our bulk sediment sampling resolution was relatively coarse (3 cm), and it is possible that sulfur gradients drive microbial diversity over smaller spatial scales. In addition, it is likely that SO_4^{2-} concentrations are so uniformly high that community composition is structured by other controllers of SO_4^{2-} reduction, like the availability of carbon and/or electron donors such as low-molecular-weight organic substrates and/or hydrogen. Even in the deepest sediments sampled (12 cm), measureable SO_4^{2-} was often detected, implying that in shallow sediments, SO_4^{2-} reduction is not limited by SO_4^{2-} availability. Regardless, microbes of the MIS sediments must be adapted to the remarkably high sulfide concentrations we measured below the mat–water interface. Hydrogen sulfide is highly toxic to most forms of aerobic life, diminishes the bioavailability and toxicity of divalent metals (Di Toro et al., 1990; Hansen et al., 2005), and can also serve as an energy source for chemosynthetic microbes (Schlesinger & Bernhardt, 2013). Thus, particularly at high concentrations, sulfide can strongly shape ecosystem structure and function (Kinsman-Costello, O'Brien, & Hamilton, 2015).

Despite the lack of broad relationships with geochemical indicators of sulfur, taxonomic markers indicate a diverse sulfur cycling microbial community in the MIS. Previous studies based on clone libraries of MIS mat and shallow sediments detected a single *Epsilonproteobacteria* and no relatives of known SRBs (Nold, Pangborn, et al., 2010). This study broadens our view of putative sulfur cycling microbial diversity in sediments. Surface mat and sediment communities both contained OTUs related to known SO_4^{2-}-reducing members of the *Deltaproteobacteria* in the *Desulfobacterales* (238 OTUs) as well as members of the sulfide-oxidizing *Epsilonproteobacteria Campylobacterales* (45 OTUs) and relatives of sulfur-oxidizing members of the genus *Beggiatoa* (14 OTUs). Metagenomic and metatranscriptomic work on MIS mat material has detected expression of known SO_4^{2-}-reduction genes in association with a *Desulfobacterales* genomic bin, and known sulfide oxidation genes associated with a *Campylobacterales* bin (Voorhies, 2014), further strengthening the evidence that members of these groups shape sulfur cycling in the sediments below as well.

Contrasting patterns of relative abundance with depth observed for putative SRB OTUs suggest niche partitioning of SO_4^{2-} reduction in this high-SO_4^{2-} environment. Although all of the notable SRB OTUs identified in the MIS and LH were members of the *Desulfobacterales*, individual OTUs displayed contrasting patterns of relative abundance. While some *Desulfobacterales* were enriched in the MIS mat, others increased in relative abundance with depth into the sediments, and some were only detected at meaningful relative abundance in LH sediments. Future work elaborating on physiological differences of OTUs that are present and functioning in different vertical zones may provide valuable information of how SO_4^{2-} supports MIS heterotrophy. Evidence continues to emerge that SO_4^{2-} reduction is not limited to specific redox zones as classically thought (Froelich et al., 1979), but can be mediated by physiologically diverse organisms in a range of environments and redox conditions (Canfield & Des Marais, 1991; Hansel et al., 2015). The high SO_4^{2-} levels present at MIS make this a valuable system in which to explore the diversity of SO_4^{2-} reduction processes and organisms.

4.1.3 | Methane cycling and archaea diversity

A picture of the MIS is emerging as a dynamic CH_4 producer and consumer. Pore water CH_4 concentrations, although higher than concentrations measured in LH pore waters, were lower than concentrations (~20 mM) previously measured in deep sediments at the MIS (Nold, Pangborn, et al., 2010). Differences in CH_4 concentrations from previous studies may be in part due to differences in sampling techniques that influence the inclusion or exclusion of gas bubbles in pore water samples. Regardless, this and previous studies demonstrate that methane concentrations in MIS decrease in shallower sediments and benthic overlying water, implying CH_4 consumption by methanotrophs in upper sediment layers and mat material. Metagenomic and transcriptomic work detected expression of a gene for CH_4 oxidation (mmoC) associated with a *Gammaproteobacteria Methylococcales* bin (Voorhies, 2014). Although we detected OTUs allied with the aerobic *Methylococcales* only at low relative abundances, declining CH_4 concentrations in shallow anoxic sediments suggest anaerobic CH_4 oxidation. Given the high availability of SO_4^{2-}, we expected to detect evidence for members of the ANME clades that pair CH_4 oxidation with SO_4^{2-} reduction (Boetius et al., 2000), yet we detected only a single OTU allied with the ANME-1 present at very low relative abundance in a handful of samples. Thus, our understanding of the MIS methanotrophic community remains limited, and it is likely that currently unknown organisms oxidize methane in this system.

Middle Island Sinkhole sediments contained an archaeal community distinct from that in LH. We detected a diverse array of OTUs at high relative abundance allied with *Woesearchaeota* and *Thermoplasmata* at high relative abundance. Relatives of these OTUs were virtually

undetected in LH sediments, implying that these *Archaea* are a distinct feature of sediments of submerged sinkhole ecosystems and not common in typical freshwater sediments. The physiological and metabolic functions of the DHVEG-6 group at MIS remain unknown, although members of this group have been detected in numerous anaerobic environments including the subsurface, saline and hypersaline lakes, and deep-sea methane seep sediments (Castelle et al., 2015; Kuroda et al., 2015; and citations therein). Recent metagenomic analysis suggests that some members of this phylum have highly reduced genomes and are specialized for a fermentative lifestyle (Castelle et al., 2015).

5 | CONCLUSIONS

Using deep microbial community sequencing and parallel geochemical characterization, we reveal a diverse and biogeochemically dynamic sediment ecosystem underlying benthic microbial mats in the MIS. In combination with data from a nearby site devoid of mat, these results provide insights into both how geochemistry promotes mat growth at MIS, and how the MIS mats influence sediment geochemistry. In this submerged Great Lake sinkhole, a vertically stratified microbial community mediates sulfur and methane cycling in a high-nutrient environment, setting the stage for the metabolically flexible surface mat above to conduct a mixture of anoxygenic photosynthesis, oxygenic photosynthesis, and chemosynthetic sulfur oxidation. These results highlight the geobiological influence of microbial mats in promoting high-nutrient flux from sediments to surface mats, establishing a positive feedback that would enhance primary productivity of microbial mats in ancient ecosystems. Future research investigating magnitudes of and controls on process rates in this distinct ecosystem will enhance our understanding of its tightly linked biogeochemistry, the causes and effects of microbial diversity, and potential biomarkers for detecting similar systems earlier on in Earth's history. Such studies have high potential to provide insight into the functioning and coevolution of microbial communities in low-oxygen microbial mat ecosystems both now and in the distant past.

ACKNOWLEDGEMENTS

We are especially grateful to the NOAA Thunder Bay National Marine Sanctuary for their support in field site access and sampling, in particular to the dive team including Russ Green, Tane Casserly, Joe Hoyt, Wayne Lusardi, Cathy Green, and Stephanie Gandulla, and ship captains Mike Taesch, Steve Bawks, and Beau Breymer. Bopi Biddanda, Michael Snider, Kathryn Gallagher, Adam McMillan, and Chelsea Mervenne assisted with field sampling, sample processing, and laboratory analyses. Special thanks to Tim Gallagher and Katy Rico for assistance in total organic C and N analysis. We gratefully acknowledge the laboratory of Dr. Steve Hamilton at Michigan State University, in particular David Weed, for providing facilities and support for ion chromatography analysis. Thanks to Tom Yavarski and the University of Michigan EWRE Aquatic Biology Lab for facilities and support in methane analysis. Funding was generously provided by the University of Michigan MCubed program, NSF grant EAR-1637066 to G.J.D., and NSF Grant EAR-1035955 to G.J.D. and N.D.S.

REFERENCES

Allen, H. E., Fu, G., Boothman, W., DiToro, D. M., & Mahoney, J. D. (1991). *Determination of acid volatile sulfides (AVS) and simultaneously extracted metals in sediment: Draft analytical method for determination of acid volatile sulfide in sediment*. Washington, DC: U.S. Environmental Protection Agency.

Anders, S., & Huber, W. (2010). Differential expression analysis for sequence count data. *Genome Biology*, *11*, R106.

Balk, M., Altinbaş, M., Rijpstra, W. I. C., Damsté, J. S. S., & Stams, A. J. M. (2008). *Desulfatirhabdium butyrativorans* gen. nov., sp. nov., a butyrate-oxidizing, sulfate-reducing bacterium isolated from an anaerobic bioreactor. *International Journal of Systematic and Evolutionary Microbiology*, *58*, 110–115.

Bates, S. T., Berg-Lyons, D., Caporaso, J. G., Walters, W. A., Knight, R., & Fierer, N. (2011). Examining the global distribution of dominant archaeal populations in soil. *The ISME Journal*, *5*, 908–917.

Battin, T. J., Kaplan, L. A., Newbold, D. J., & Hansen, C. M. E. (2003). Contributions of microbial biofilms to ecosystem processes in stream mesocosms. *Nature*, *426*, 439–442.

Benjamini, Y., & Hochberg, Y. (1995). Controlling the false discovery rate: A practical and powerful approach to multiple testing. *Journal of the Royal Statistical Society. Series B (Methodological)*, *57*, 289–300.

Biddanda, B. A., Coleman, D. F., Johengen, T. H., Ruberg, S. A., Meadows, G. A., Van Sumeren, H. W., … Kendall, S. T. (2006). Exploration of a submerged sinkhole ecosystem in Lake Huron. *Ecosystems*, *9*, 828–842.

Biddanda, B. A., McMillan, A. C., Long, S. A., Snider, M. J., & Weinke, A. D. (2015). Seeking sunlight: Rapid phototactic motility of filamentous mat-forming cyanobacteria optimize photosynthesis and enhance carbon burial in Lake Huron's submerged sinkholes. *Frontiers in Microbiology*, *6*, 1–13.

Biddanda, B. A., Nold, S. C., Ruberg, S. A., Kendall, S. T., Sanders, T. G., & Gray, J. J. (2009). Great Lakes Sinkholes: A Microbiogeochemical Frontier. *EOS, Transactions, American Geophysical Union*, *90*, 62–69.

Boetius, A., Ravenschlag, K., Schubert, C. J., Rickert, D., Widdel, F., Gieseke, A., … Pfannkuche, O. (2000). A marine microbial consortium apparently mediating anaerobic oxidation of methane. *Nature*, *407*, 623–626.

Bogorad, L. (1975). Phycobiliprotein: Complementary chromatic adaptation. *Annual Review of Plant Physiology*, *26*, 369–401.

Camacho, A., Vicente, E., & Miracle, M. R. (2000). Ecology of a deep-living *Oscillatoria (=Planktothrix)* population in the sulphide-rich waters of a Spanish karstic lake. *Archiv fur Hydrobiologie*, *148*, 333–355.

Canfield, D. E., & Des Marais, D. J. (1991). Aerobic sulfate reduction in microbial mats. *Science*, *251*, 1471–1473.

Canfield, D. E., & Des Marais, D. J. (1993). Biogeochemical cycles of carbon, sulfur, and free oxygen in a microbial mat. *Geochimica et cosmochimica acta*, *57*, 3971–3984.

Castelle, C. J., Wrighton, K. C., Thomas, B. C., Hug, L. A., Brown, C. T., Wilkins, M. J., … Banfield, J. F. (2015). Genomic expansion of domain archaea highlights roles for organisms from new phyla in anaerobic carbon cycling. *Current Biology*, *25*, 690–701.

Clarke, K. R. (1993). Non-parametric multivariate analyses of changes in community structure. *Australian Journal of Ecology*, *18*, 117–143.

Decho, A. W. (1990). Microbial exopolymer secretions in ocean environments: Their role(s) in food webs and marine processes. *Oceanography and Marine Biology Annual Review*, *28*, 73–153.

Di Toro, D. M., Mahony, J. D., Hansen, D. J., Scott, K. J., Hicks, M. B., Mayr, S. M., & Redmond, M. S. (1990). Toxicity of cadmium in sediments: The role of acid volatile sulfide. *Environmental Toxicology and Chemistry*, *9*, 1487–1502.

Edgar, R. C. (2013). UPARSE: Highly accurate OTU sequences from microbial amplicon reads. *Nature Methods*, *10*, 996–998.

Faith, D. P. (1992). Conservation evaluation and phylogenetic diversity. *Biological Conservation*, *61*, 1–10.

Finster, K., Liesack, W., & Thamdrup, B. (1998). Elemental sulfur and thiosulfate disproportionation by Desulfocapsa sulfoexigens sp. nov., a new anaerobic bacterium isolated from marine surface sediment. *Applied and Environmental Microbiology*, *64*, 119–125.

Froelich, P. N., Klinkhammer, G. P., Bender, M. L., Luedtke, N. A., Heath, G. R., Cullen, D., & Dauphin, P. (1979). Early oxidation of organic matter in pelagic sediments of the eastern equatorial Atlantic: Suboxic diagenesis. *Geochimica et Cosmochimica Acta*, *43*, 1075–1090.

Hansel, C. M., Lentini, C. J., Tang, Y., Johnston, D. T., Wankel, S. D., & Jardine, P. M. (2015). Dominance of sulfur-fueled iron oxide reduction in low-sulfate freshwater sediments. *The ISME Journal*, *9*, 2400–2412.

Hansen, D., Di Toro, D. M., Berry, W., Boothman, W., McGrath, J., & Ankley, G. T. (2005). Procedures for the derivation of equilibrium partitioning sediment benchmarks (ESBs) for the protection of benthic organisms: Metal mixtures (cadmium, copper, lead, nickel, silver and zinc). EPA 600/R-02/011. US Environmental Protection Agency, Washington, DC.

Hayes, J. M., & Waldbauer, J. R. (2006). The carbon cycle and associated redox processes through time. *Philosophical Transactions of the Royal Society B: Biological Sciences*, *361*, 931–950.

Hoehler, T. M., Bebout, B. M., & Des Marais, D. J. (2001). The role of microbial mats in the production of reduced gases on the early Earth. *Nature*, *412*, 324–327.

Jeroschewski, P., Steuckart, C., & Kühl, M. (1996). An amperometric microsensor for the determination of H_2S in aquatic environments. *Analytical Chemistry*, *68*, 4351–4357.

Kembel, S. W., Cowan, P. D., Helmus, M. R., Cornwell, W. K., Morlon, H., Ackerly, D. D., … Webb, C. O. (2010). Picante: R tools for integrating phylogenies and ecology. *Bioinformatics*, *26*, 1463–1464.

Kinsman-Costello, L. E., O'Brien, J. M., & Hamilton, S. K. (2015). Natural stressors in uncontaminated sediments of shallow freshwaters: The prevalence of sulfide, ammonia, and reduced iron. *Environmental Toxicology and Chemistry*, *34*, 467–479.

Klatt, J. M., Haas, S., Yllmaz, P., de Beer, D., & Polerecky, L. (2015). Hydrogen sylfide can inhibit and enhance oxygenic photosynthesis in a cyanobacterium from sulfidic springs. *Environmental Microbiology*, *17*, 3301–3313.

Kozich, J. J., Westcott, S. L., Baxter, N. T., Highlander, S. K., & Schloss, P. D. (2013). Development of a dual-index sequencing strategy and curation pipeline for analyzing amplicon sequence data on the MiSeq Illumina sequencing platform. *Applied and Environmental Microbiology*, *79*, 5112–5120.

Kromkamp, J. (1987). Formation and functional significance of storage products in cyanobacteria. *New Zealand Journal of Marine and Freshwater Research*, *21*, 457–465.

Kühl, M., & Revsbech, N. P. (2001). Biogeochemical microsensors for boundary layer studies. In B. P. Boudrew, & B. B. Jørgensen (Eds.), *The benthic boundary layer* (pp. 180–210). New York, NY, USA: Oxford University Press.

Kuroda, K., Hatamoto, M., Nakahara, N., Abe, K., Takahashi, M., Araki, N., & Yamaguchi, T. (2015). Community composition of known and uncultured archaeal lineages in anaerobic or anoxic wastewater treatment sludge. *Microbial Ecology*, *69*, 586–596.

Lalonde, S. V., & Konhauser, K. O. (2015). Benthic perspective on Earth's oldest evidence for oxygenic photosynthesis. *Proceedings of the National Academy of Sciences, USA*, *112*, 995–1000.

Luque, I., Zabulon, G., Contreras, A., & Houmard, J. (2001). Convergence of two global transcriptional regulators on nitrogen induction of the stress-acclimation gene nblA in the cyanobacterium *Synechococcus* sp. PCC 7942. *Molecular Microbiology*, *41*, 937–947.

Macalady, J. L., Lyon, E. H., Koffman, B., Albertson, L. K., Meyer, K., Galdenzi, S., & Mariani, S. (2006). Dominant microbial populations in limestone-corroding stream biofilms, Frasassi cave system, Italy. *Applied and Environmental Microbiology*, *72*, 5596–5609.

Matheron, R., & Caumette, P. (2015). Structure and functions of microorganisms: Production and use of material and energy. In J.-C. Bertrand, P. Caumette, P. Lebaron, R. Matheron, P. Normand, & T. Sime-Ngando (Eds.), *Environmental microbiology: Fundamentals and applications*, (pp. 25–75). Dordrecht, the Netherlands: Springer.

McMurdie, P. J., & Holmes, S. (2014). Waste not, want not: Why rarefying microbiome data is inadmissible. *PLoS Computational Biology*, *10*, e1003531.

Megonigal, J. P., Hines, M. E., & Visscher, P. T. (2004). Anaerobic metabolism: Linkages to trace gases and aerobic processes. In W. H. Schlesinger (Ed.), *Biogeochemistry* (pp. 317–424). Oxford, UK: Elsevier-Pergamon.

Murphy, J., & Riley, J. P. (1962). A modified single solution method for the determination of phosphate in natural waters. *Analytica Chimica Acta*, *27*, 31–36.

Nimick, D. A., Gammons, C. H., Cleasby, T. E., Madison, J. P., Skaar, D., & Brick, C. M. (2003). Diel cycles in dissolved metal concentrations in streams: Occurrence and possible causes. *Water Resources Research*, *39*, 1247.

Nold, S. C., Bellecourt, M. J., Kendall, S. T., Ruberg, S. A., Sanders, T. G., Klump, J. V., & Biddanda, B. A. (2013). Underwater sinkhole sediments sequester Lake Huron's carbon. *Biogeochemistry*, *115*, 235–250.

Nold, S. C., Pangborn, J. B., Zajack, H. A., Kendall, S. T., Rediske, R. R., & Biddanda, B. A. (2010). Benthic bacterial diversity in submerged sinkhole ecosystems. *Applied and Environmental Microbiology*, *76*, 347–351.

Nold, S. C., Zajack, H. A., & Biddanda, B. A. (2010). Eukaryal and archaeal diversity in a submerged sinkhole ecosystem influenced by sulfur-rich, hypoxic groundwater. *Journal of Great Lakes Research*, *36*, 366–375.

Paerl, H. W., Pinckney, J. L., & Steppe, T. F. (2000). Cyanobacterial-bacterial mat consortia: Examining the functional unit of microbial survival and growth in extreme environments. *Environmental Microbiology*, *2*, 11–26.

Price, M. N., Dehal, P. S., & Arkin, A. P. (2009). FastTree: Computing large minimum evolution trees with profiles instead of a distance matrix. *Molecular Biology and Evolution*, *26*, 1641–1650.

Pruesse, E., Quast, C., Knittel, K., Fuchs, B. M., Ludwig, W., Peplies, J., & Glöckner, F. O. (2007). SILVA: A comprehensive online resource for quality checked and aligned ribosomal RNA sequence data compatible with ARB. *Nucleic Acids Research*, *35*, 7188–7196.

R Core Team (2015) *R: A language and environment for statistical computing*. Vienna, Austria: R Foundation for Statistical Computing. URL https://www.R-project.org/

Revsbech, N. P. (1989). An oxygen microsensor with a guard cathode. *Limnology & Oceanography*, *34*, 474–478.

Ruberg, S. A., Coleman, D. F., Johengen, T. H., Meadows, G. A., VanSumeren, H. W., Lang, G. A., & Biddanda, B. A. (2005). Groundwater plume mapping in a submerged sinkhole in Lake Huron. *Marine Technology Society Journal*, *39*, 65–69.

Ruberg, S. A., Kendall, S. T., Biddanda, B. A., Black, T., Nold, S. C., Lusardi, W. R., … Constant, S. A. (2008). Observations of the Middle Island Sinkhole in Lake Huron – A unique hydrogeologic and glacial creation of 400 million years. *Marine Technology Society Journal*, *42*, 12–21.

Sanders, T. G. J., Biddanda, B. A., Stricker, C. A., & Nold, S. C. (2011). Benthic macroinvertebrate and fish communities in Lake Huron are linked to submerged groundwater vents. *Aquatic Biology*, *12*, 1–12.

Schlesinger, W. H., & Bernhardt, E. S. (2013). *Biogeochemistry: An analysis of global change* (3rd ed.). Waltham, MA: Academic Press.

Schloss, P. D., Westcott, S. L., Ryabin, T., Hall, J. R., Hartmann, M., Hollister, E. B., … Weber, C. F. (2009). Introducing mothur: Open-source, platform-independent, community-supported software for describing and comparing microbial communities. *Applied and Environmental Microbiology*, *75*, 7537–7541.

Stal, L. J. (1995). Tansley Review No. 84 Physiological ecology of cyanobacteria in microbial mats and other communities. *New Phytologist*, *131*, 1–32.

Sumner, D. Y., Hawes, I., Mackey, T. J., Jungblut, A. D., & Doran, P. T. (2015). Antarctic microbial mats: A modern analog for Archean lacustrine oxygen oases. *Geology*, *43*, 887–890.

Voorhies, A. A. (2014). Investigation of microbial interactions and ecosystem dynamics in a low O2 cyanobacterial mat. Doctoral dissertation, University of Michigan.

Voorhies, A. A., Biddanda, B. A., Kendall, S. T., Jain, S., Marcus, D. N., Nold, S. C., … Dick, G. J. (2012). Cyanobacterial life at low O_2: Community genomics and function reveal metabolic versatility and extremely low diversity in a Great Lakes sinkhole mat. *Geobiology*, *10*, 250–267.

Voorhies, A. A., Eisenlord, S. D., Marcus, D. N., Duhaime, M. B., Biddanda, B. A., Cavalcoli, J. D., & Dick, G. J. (2016). Ecological and genetic interactions between cyanobacteria and viruses in a low-oxygen mat community inferred through metagenomics and metatranscriptomics. *Environmental Microbiology*, *18*, 358–371.

Wang, Q., Garrity, G. M., Tiedje, J. M., & Cole, J. R. (2007). Naive Bayesian classifier for rapid assignment of rRNA sequences into the new bacterial taxonomy. *Applied and Environmental Microbiology*, 73, 5261–5267.

SUPPORTING INFORMATION

Additional Supporting Information may be found online in the supporting information tab for this article.